

Gradient corrections to the exchange-correlation free energy

Travis Sjoström and Jérôme Daligault

Theoretical Division, Los Alamos National Laboratory, Los Alamos, New Mexico 87545, USA

(Received 6 August 2014; revised manuscript received 22 September 2014; published 7 October 2014)

We develop the first-order gradient correction to the exchange-correlation free energy of the homogeneous electron gas for use in finite-temperature density functional calculations. Based on this, we propose and implement a simple temperature-dependent extension for functionals beyond the local density approximation. These finite-temperature functionals show improvement over zero-temperature functionals, as compared to path-integral Monte Carlo calculations for deuterium equations of state, and perform without computational cost increase compared to zero-temperature functionals and so should be used for finite-temperature calculations. While the present functionals are valid at all temperatures including zero, non-negligible difference with zero-temperature functionals begins at temperatures above 10 000 K.

DOI: [10.1103/PhysRevB.90.155109](https://doi.org/10.1103/PhysRevB.90.155109)

PACS number(s): 71.15.Mb, 31.15.E–, 05.70.Ce

I. INTRODUCTION

The understanding of matter in extreme conditions represents a significant and current challenge of high-energy density physics [1,2]. Some particular systems of interest include dense astrophysical plasmas, which exist in the interiors of giant planets, as well as warm dense matter, which is increasingly studied in high-energy density laboratory experiments. In these conditions of elevated temperature and density relative to the ambient condensed-matter state, ions can be strongly coupled and electrons are at least partially degenerate. These conditions have proven difficult to describe theoretically and necessitate numeric simulations [3].

One key approach is molecular dynamics simulations via density functional theory (DFT). In this approach, the ions are treated classically and propagated according to Newton's equations, where the force is determined from the ions' interaction with each other and the electron density. The electron density is solved for at each ionic configuration in accord with the Born-Oppenheimer approximation using DFT methods. In particular, the electron free energy is minimized subject to conservation of the number of electrons in order to determine the electron density. This free energy is given by the density functional

$$F[n] = F_s[n] + F_H[n] + F_{xc}[n] + F_{ei}[n], \quad (1)$$

where F_s is the noninteracting free energy comprised of both kinetic and entropic parts, F_H is the Hartree energy or direct Coulomb interaction between the electrons, F_{ei} is the electron-ion Coulomb interaction, and F_{xc} is defined as the remainder of the total free energy, which includes the quantum mechanical exchange and correlation as well as the excess kinetic and entropic terms. F_{xc} is a key contribution for which there is not an exact expression and, hence, it must be approximated by a density functional that is, in general, temperature dependent. However, while the DFT approach is increasingly used to study higher-temperature systems [4–6], zero-temperature exchange-correlation functionals are most commonly employed, even at significant temperature, as opposed to explicitly temperature-dependent functionals.

Recently, fits were provided for F_{xc} in the local density approximation (LDA) [7], which is the simplest type of density functional. At zero temperature, the LDA has seen significant

improvements made upon it over the past 40 years. In the first step beyond LDA, density gradient expansions were examined, then generalized gradient approximations were developed, and later even more complex, orbital-dependent functionals were considered [8,9]. While a similar effort has not been seen at finite temperature, Geldart and co-workers [10] did derive the gradient expansion for the exchange-only contribution. In this paper, we examine the gradient expansion for the full exchange-correlation functional and, based on that, provide a simple finite-temperature extension for generalized gradient functionals. In addition, we perform self-consistent calculations to determine the overall importance of temperature dependence in exchange-correlation functionals.

II. GRADIENT CORRECTIONS TO THE EXCHANGE-CORRELATION FREE ENERGY**A. Development of the gradient expansion**

In order to determine the gradient expansion, we consider the relation of density functional theory to dielectric theory for the uniform electron gas. Following Kohn and Sham, we first write the gradient expansion of the exchange-correlation free energy as

$$F_{xc}[n] = \int d\mathbf{r} f_{xc}(n, T)n(\mathbf{r}) + \frac{1}{2} \int d\mathbf{r} g_{xc}^{(2)}(n, T)|\nabla n(\mathbf{r})|^2 + \dots, \quad (2)$$

where n and T are the electron density and temperature, respectively. The first term of the right-hand side on its own is the local density approximation, with f_{xc} the exchange-correlation free energy per electron in the uniform electron gas. The coefficient of the gradient correction term, $g_{xc}^{(2)}$, is the piece determined in this work, and it is related to the static local field correction $G(k)$ of the homogeneous electron gas by [11–14]

$$g_{xc}^{(2)}(n, T) = \frac{1}{2} \left(\frac{\partial^2[-v_k G(k)]}{\partial k^2} \right)_{k \rightarrow 0} = -4\pi e^2 \delta / k_F^4, \quad (3)$$

where $v_k = 4\pi e^2/k^2$ is the Coulomb potential, $k_F = (3\pi^2 n)^{1/3}$, and in the second line we consider the small- k expansion of $G(k) = \gamma(k/k_F)^2 + \delta(k/k_F)^4 + \dots$. Here the dependence of G , γ , and δ on n and T is suppressed for convenience.

It is known that G may be well represented for small and large k , though not for intermediate values, by the function [15,16]

$$G(q) = A(1 - e^{Bq^2}), \quad (4)$$

with $q = k/k_F$. Then, for small q ,

$$G(q) = ABq^2 - \frac{1}{2}AB^2q^4 + \dots, \quad (5)$$

and so

$$\gamma = AB, \quad \delta = -AB^2/2. \quad (6)$$

Next, from the compressibility sum rule, we have

$$\gamma = -\frac{k_F^2}{4\pi e} \frac{\partial^2(nf_{xc})}{\partial n^2}, \quad (7)$$

which we may evaluate by the recent analytic fits [7] for f_{xc} that are based on the quantum Monte Carlo (QMC) data [17] for the internal exchange-correlation energies of the homogeneous electron gas at finite temperatures. This leaves us still needing A or B independently to determine δ and hence $g_{xc}^{(2)}$. This is completed then by the relation for the large- q limit of $G(q)$ to the pair-distribution function [18], $g(r)$,

$$A = G(q \rightarrow \infty) = 1 - g(0). \quad (8)$$

In order to determine the gradient coefficient, we now need only $g(0)$ further (again T and n dependence is suppressed). This we obtain from the same QMC results of Brown *et al.* [17] that the f_{xc} fit is based on, in which they also provide $g(r)$ for the unpolarized system. However, their grid does not include $g(0)$ so we have extrapolated their $g(r)$ data to obtain $g(0)$ by fitting $g(r) = a + ar + br^2$ for small r , in accord with the cusp condition [19] at each density and temperature point given in the QMC results. Next we perform a separate fit for $g(0)$ as a function of r_s at each temperature $t = k_B T/E_F = \{0.0625, 0.125, 0.25, 0.5, 1.0, 2.0, 4.0, 8.0\}$, according to the following equation [20]:

$$g(0) = \frac{1}{2} \frac{1 + a\sqrt{r_s} + br_s}{1 + cr_s + dr_s^3}. \quad (9)$$

The fit results are plotted for selected t in the upper panel of Fig. 1 along with the $g(0)$ extrapolated from the QMC data. Then, using Eqs. (3)–(8) along with the fits for $g(0)$, we find $g_{xc}^{(2)}$ as a function of r_s for the given t values. The results are plotted for $t = 0.0625, 1, 4, 8$ in the lower panel of Fig. 1. It is worth noting that the $g(0)$ curve for $t = 0.0625$ is nearly identical to that for the $t = 0$ QMC result of Spink *et al.* [20].

B. Analysis of the temperature dependence

To examine the effects of the temperature-dependent gradient coefficient $g_{xc}^{(2)}$, we calculate its relative contributions on various systems at different temperatures and densities. Specifically, we solve all electron hydrogen, aluminum, and iron systems at each t for which we have fit $g_{xc}^{(2)}$ and at selected densities from ambient to several times ambient compression.

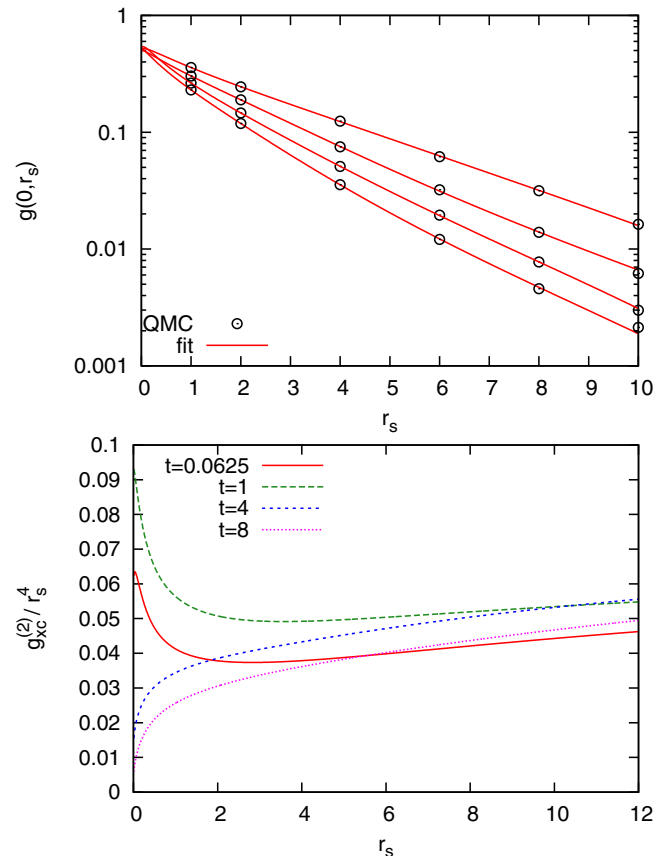


FIG. 1. (Color online) Top: QMC data points for $g(0)$ and our fit as a function of r_s for a given $t = k_B T/E_F$, with the curves being $t = 8, 4, 0.0625, 1$ from top to bottom. Bottom: Coefficient of the gradient expansion $g_{xc}^{(2)}$, for given t as derived from QMC fits for f_{xc} [7] and $g(0)$ (top).

We first solve the system in an average atom model [21] using an orbital-free functional for the noninteracting contribution, namely, the finite-temperature Thomas-Fermi plus von Weizsäcker approximation [22], and a zero-temperature LDA for the exchange-correlation energy. The average atom model consists of a nucleus at the center of a spherical cavity of volume that is determined by prescribing the density of the material. The spherically symmetric electron density is then found by density functional theory, subject to the condition that the integrated electron density in the cavity is equal to the charge of the nucleus. This gives us a realistic average density around each ion. Then, using this density, we evaluate the different exchange-correlation free-energy contributions to determine their relative effects, with the results shown in Fig. 2. The relative effect of the temperature dependence of the local density term is shown in the red curves given by

$$\frac{\int d\mathbf{r} n(f_{xc} - \epsilon_{xc})}{\int d\mathbf{r} n \epsilon_{xc}}, \quad (10)$$

where $\epsilon_{xc} = f_{xc}(t=0)$ is the zero-temperature exchange-correlation energy, while the total relative contribution due to the gradient term as well as that portion due to its

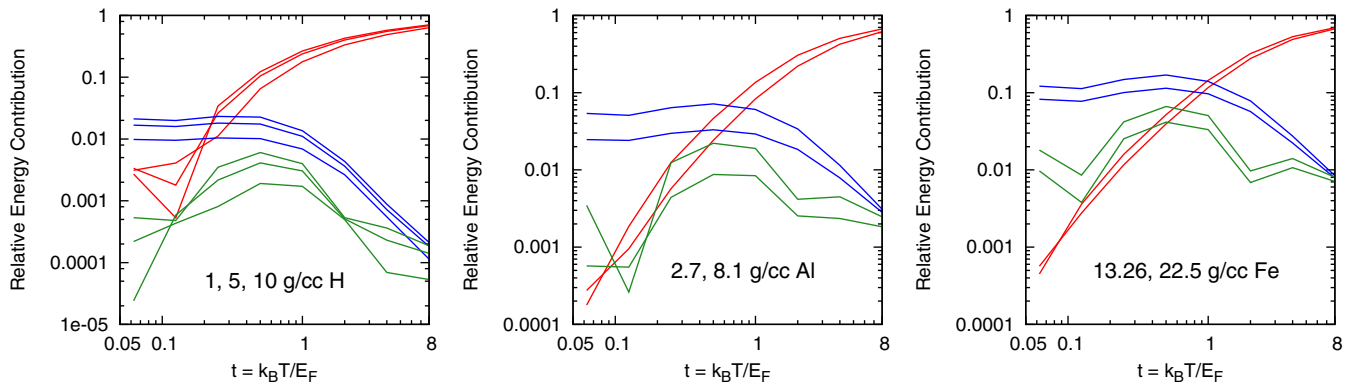


FIG. 2. (Color online) Relative effects of the terms of the gradient expansion for the exchange-correlation free energy. The temperature dependence of the local density term becomes dominant at high temperatures [red curves, Eq. (10)] and the gradient term is most important at lower temperatures [blue curves, Eq. (11)], while the temperature dependence of the gradient term is always negligible [green curves, Eq. (12)]. Different curves of the same color represent the different densities.

finite-temperature contribution are given by

$$\frac{\int d\mathbf{r} |\nabla n|^2 g_{xc}^{(2)} / 2}{\int d\mathbf{r} n f_{xc}}, \quad (11)$$

$$\frac{\int d\mathbf{r} |\nabla n|^2 [g_{xc}^{(2)}(t) - g_{xc}^{(2)}(t=0)] / 2}{\int d\mathbf{r} n f_{xc}}, \quad (12)$$

and are shown in the blue and green curves, respectively. These results show that at high temperature, the dependence of the local density term provides the dominant correction; however, at low temperature, the gradient correction is most important. By comparison, the temperature-dependent correction coming from the gradient term is always negligible. This is not unexpected when considering Fig. 1, where for $g_{xc}^{(2)}$ although the different temperature curves do vary, they remain relatively close to the lowest-temperature case for all t .

C. Beyond the gradient expansion

In considering an improved gradient corrected functional for the exchange-correlation free energy, we reiterate that the previous analysis shows that temperature dependence in the gradient term is, in fact, negligible. That is, using a zero-temperature gradient correction at finite temperature is in fact a good approximation. However, this applies only to the gradient term; the local density term does show a significant temperature dependence and a proper finite-temperature functional should be used in that case. It is also clear, though, that gradient corrections are important at low temperature. Beyond this generality, it is well known from zero-temperature development that gradient expansions for the exchange correlation yield poor results that are often no better or worse than the local density approximation [11,23,24]. Generalized gradient approximations (GGAs), such as Perdew-Burke-Ernzerhof (PBE) [25], have proven to perform significantly better than gradient expansions at zero temperature. Given the quality GGA's available at zero temperature and with our current analysis of the gradient corrections *nontemperature* dependence, we therefore propose a temperature-dependent

GGA as follows:

$$F_{xc}^{GGA}[n] = E_{xc}^{GGA}[n] - E_{xc}^{LDA}[n] + F_{xc}^{LDA}[n]. \quad (13)$$

Here the zero-temperature GGA term $E_{xc}^{GGA}[n]$ includes the local density contribution. Then the zero-temperature local density contribution is removed and replaced with the finite-temperature version, thus capturing all significant temperature and density gradient dependence in the exchange-correlation free energy.

D. Self-consistent results

We have implemented the finite-temperature exchange-correlation free energy both in the local density approximation, as given in Ref. [7], as well as in the finite-temperature modification of the zero-temperature PBE functional according to Eq. (13) in the plane-wave density-functional-theory code QUANTUM ESPRESSO [26] and in our orbital-free code. We

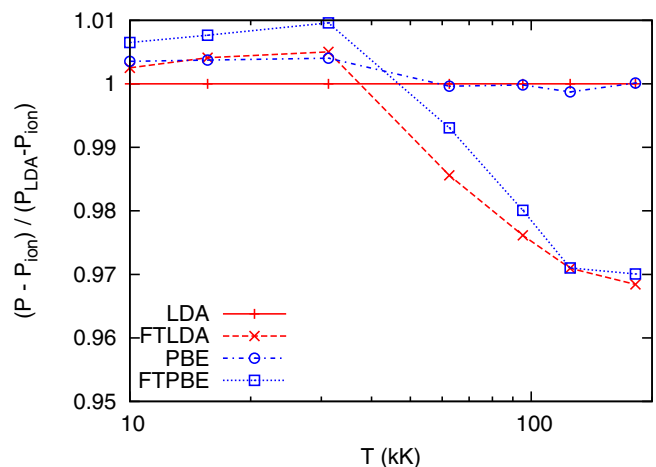


FIG. 3. (Color online) Deuterium pressure, excluding the ion kinetic contribution, at 4.05 g/cc for the LDA and GGA functionals with and without temperature dependence plotted relative to the zero-temperature LDA results. The increased significance of the temperature-dependent functionals and the decreased effect from the gradient terms for higher temperatures are shown.

then applied this to cases of warm dense deuterium, for which there exist path-integral Monte Carlo (PIMC) equation-of-state results [27] that do not require an approximate input for the exchange-correlation free energy.

Specifically, we ran both Kohn-Sham and orbital-free DFT-based molecular dynamics simulations for warm dense deuterium. For the Kohn-Sham calculations, a nonlocal pseudopotential was used and a local pseudopotential was used for the orbital-free calculations; these are as given in Ref. [22]. The orbital-free functional is that given in Ref. [28]. In both cases, 128 atoms were simulated with periodic boundary conditions for at least 5000 time steps, where the time step varied from 0.5 fs at 10 kK to 0.0125 fs at 1000 kK (1000 K = 1 kK). Also, only the Γ point was used in the Kohn-Sham calculations.

In Fig. 3, we plot the resulting pressure relative to the pressure from a zero-temperature LDA calculation for deuterium at 4.05 g/cc and up to nearly 200 kK, where we have subtracted out the ion kinetic pressure, $P_{\text{ion}} = N_{\text{ion}}k_B T/V$. Using the standard zero-temperature PBE, it is clear that the gradient correction becomes less and less as temperature increases. In contrast, both finite-temperature functionals first show a small increase in pressure at low temperature, then a more significant decrease in pressure as

the temperature is elevated to 200 kK. This can be understood in terms of f_{xc} , which is always negatively valued. For a given density, f_{xc} becomes slightly more negative to a minimum, and then increases towards zero as temperature becomes very high. The net result at high temperature then is to reduce the exchange-correlation contribution to the pressure. Again we note that the gradient effects diminish with increasing temperature.

In order to consider the temperature effect in the warm dense regime, we consider just the LDA functional for deuterium at 4.05 g/cc and at 10.0 g/cc. These results are shown in Fig. 4 along with the PIMC data [27]. In order to extend the calculation from 200 kK up to 1000 kK in temperature, we make use of an orbital-free density functional calculation. The plotted results are then the total pressure relative to the total pressure from a zero-temperature LDA exchange-correlation calculation in either Kohn-Sham or orbital-free (OF) method, and hence the LDA and OF LDA curves are exactly one. Note that the PIMC results are shown relative to OF LDA. The orbital-free method is seen to be justified as here it overlaps

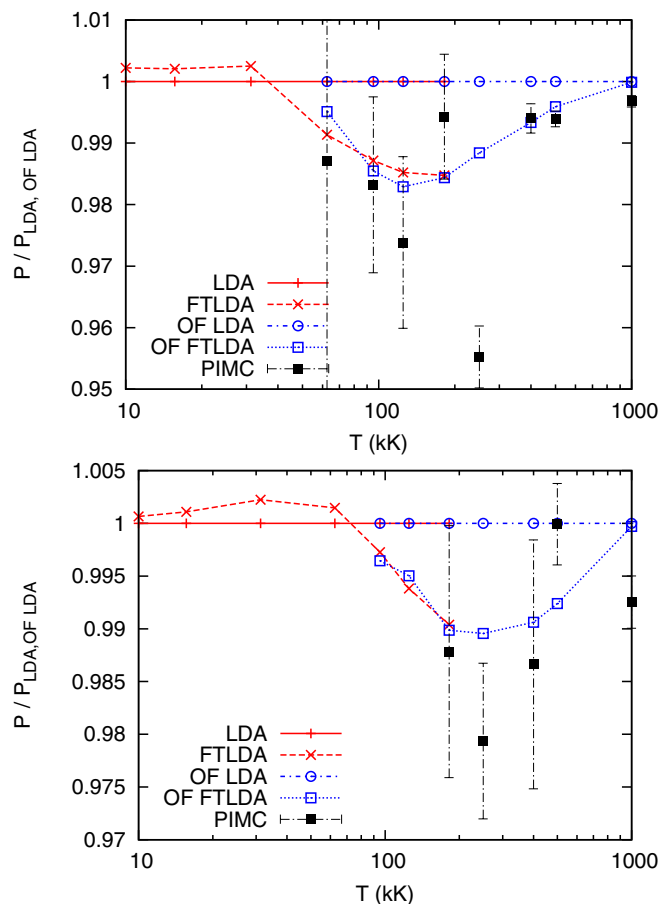


FIG. 4. (Color online) Deuterium pressure at 4.05 g/cc (top) and 10.0 g/cc (bottom) for the LDA functional with and without temperature dependence, as well as PIMC results, relative to the zero-temperature LDA results. At both densities, the temperature-dependent functional agrees better with the PIMC.

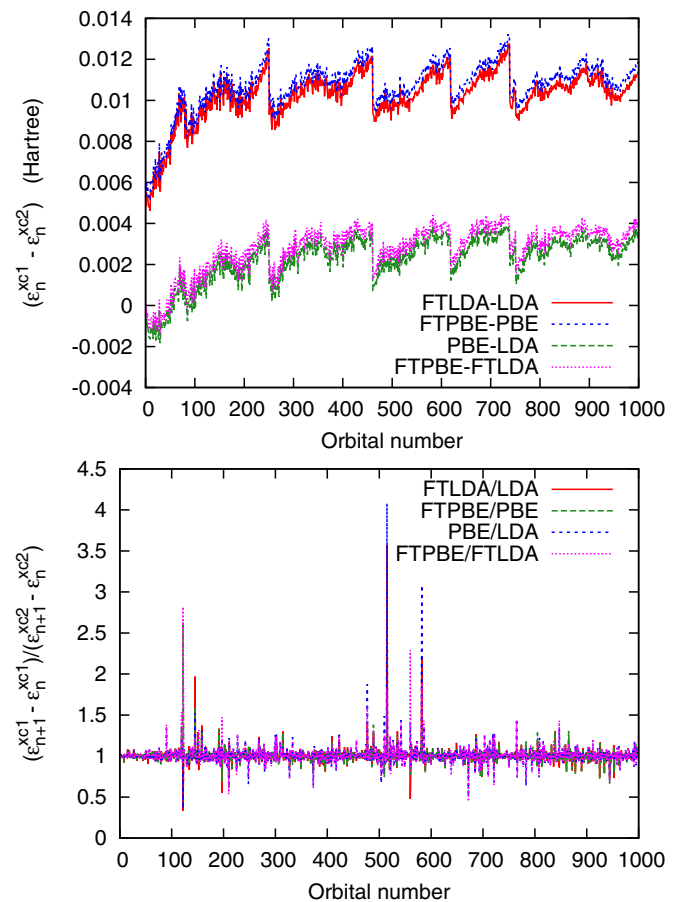


FIG. 5. (Color online) Differences in corresponding eigenvalue energies between two different exchange-correlation functionals (upper panel) and the ratio of adjacent eigenvalue differences for two functionals (lower panel) are shown for 128 deuterium atoms at 4.05 g/cc and 181.8 kK. The two functional combinations are given in the plot legend. There is a non-negligible difference which arises from inclusion of the finite-temperature contribution to the exchange-correlation energy.

well with the highest-temperature Kohn-Sham calculations. These relative pressure results do show better agreement of the temperature-dependent functional with that of the PIMC results versus those of the zero-temperature functional at both densities. We can see in these cases that there is a maximum difference of 1–2% in the total pressure in the warm dense regime. This effect then diminishes to zero at high temperatures as the total exchange-correlation contribution to the pressure becomes completely negligible compared to the kinetic contributions of the electrons and ions.

Finally, we consider the effect of temperature-dependent exchange correlation on the eigenspectrum of a real system. In the upper panel of Fig. 5, for a single random configuration of 128 deuterium atoms at 4.05 g/cc and 181.8 kK, we plot the difference in corresponding eigenvalues when using different functionals. The difference between finite-temperature and zero-temperature functionals here produces about a five-times-greater difference than the difference between PBE and LDA whether in the finite-temperature or zero-temperature versions. In the lower panel, the ratio of adjacent eigenvalue differences, $(\epsilon_{n+1} - \epsilon_n)$, is taken between the different functionals. The average is clearly seen to always be 1, but there is non-negligible spread seen, which is quantified by the standard deviation of 0.12 and 0.09 for the finite-temperature to zero-temperature functional results of LDA and PBE, respectively, and 0.15 and 0.12 for the PBE to LDA results for zero-temperature and finite-temperature functionals, respectively. The significance in addressing the eigenspectrum is that these orbitals (eigenfunctions) and eigenvalues are directly used in various calculations such as for the electrical conductivity through the Kubo-Greenwood formalism, in which the differences in energy levels are required. Here we have shown that the primary effect of the temperature-dependent exchange correlation is to shift the eigenspectrum; however, there are also changes in the relative spacing. Though we

have not performed such calculations here, we suggest that such orbital-dependent calculations may also be affected by temperature-dependent exchange correlation.

III. SUMMARY

We have derived the finite-temperature gradient expansion for the exchange-correlation free energy and then demonstrated that the contribution from the temperature dependence of the gradient term in physical systems is negligible. However, the gradient corrections are important at lower temperatures and the finite-temperature correction to the local density contribution is important at higher temperatures. We therefore proposed a temperature-dependent GGA and showed that the temperature dependence is more significant than gradient dependence in the warm dense matter regime and that better results are achieved using temperature-dependent LDA or GGA, as shown by better agreement with PIMC equation-of-state data for which there is no approximation for the exchange-correlation energy. Finally, these finite-temperature corrections are easily implemented in any DFT code, through the fit given in Ref. [7], and perform without computational cost increase and so should be used for finite-temperature calculations where better accuracy is desired. We do note that though these finite-temperature functionals are valid down to and including zero, for most condensed-matter systems below 10 000 K, little to no differences will be seen as compared with using zero-temperature exchange-correlation functionals.

ACKNOWLEDGMENTS

This work was carried out under the auspices of the National Nuclear Security Administration of the U.S. Department of Energy (DOE) at Los Alamos National Laboratory under Contract No. DE-AC52-06NA25396. The work was supported by the DOE Office of Fusion Sciences.

-
- [1] R. P. Drake, *Phys. Today* **63**, 28 (2010).
 - [2] T. Rothman (ed.), *Basic Research Needs for High Energy Density Laboratory Physics*, Report on the Workshop on High Energy Density Laboratory Physics Research Needs, Nov. 15–18, 2009 (U.S. Department of Energy, Office of Science and National Nuclear Security Administration, Washington, D.C., 2010).
 - [3] F. Graziani, M. P. Desjarlais, R. Redmer, and S. B. Trickey (eds.), *Frontiers and Challenges in Warm Dense Matter*, Lecture Notes in Computational Science and Engineering Vol. 96 (Springer, Berlin, 2014).
 - [4] M. P. Desjarlais, J. D. Kress, and L. A. Collins, *Phys. Rev. E* **66**, 025401(R) (2002).
 - [5] K. P. Driver and B. Militzer, *Phys. Rev. Lett.* **108**, 115502 (2012).
 - [6] C. Wang and P. Zhang, *Phys. Plasmas* **20**, 092703 (2013).
 - [7] V. V. Karasiev, T. Sjostrom, J. Dufty, and S. B. Trickey, *Phys. Rev. Lett.* **112**, 076403 (2014).
 - [8] J. P. Perdew and K. Schmidt, *AIP Conf. Proc.* **577**, 1 (2001).
 - [9] A. D. Becke, *J. Chem. Phys.* **140**, 18A301 (2014).
 - [10] E. Dunlap and D. J. W. Geldart, *Can. J. Phys.* **72**, 1 (1994); M. L. Glasser, D. J. W. Geldart, and E. Dunlap, *ibid.* **72**, 7 (1994); M. R. A. Shegelski, D. J. W. Geldart, M. L. Glasser, and D. Nielson, *ibid.* **72**, 14 (1994).
 - [11] A. K. Gupta and K. S. Singwi, *Phys. Rev. B* **15**, 1801 (1977).
 - [12] G. Niklasson, A. Sjölander, and K. S. Singwi, *Phys. Rev. B* **11**, 113 (1975).
 - [13] W. Kohn and L. J. Sham, *Phys. Rev.* **140**, A1133 (1965).
 - [14] P. Hohenberg and W. Kohn, *Phys. Rev.* **136**, B864 (1964).
 - [15] P. Vashista and K. S. Singwi, *Phys. Rev. B* **6**, 875 (1972).
 - [16] R. G. Dandrea, N. W. Ashcroft, and A. E. Carlsson, *Phys. Rev. B* **34**, 2097 (1986).
 - [17] E. W. Brown, B. K. Clark, J. L. DuBois, and D. M. Ceperley, *Phys. Rev. Lett.* **110**, 146405 (2013).
 - [18] S. Tanaka and S. Ichimaru, *J. Phys. Soc. Jpn.* **55**, 2278 (1986).
 - [19] J. C. Kimball, *Phys. Rev. A* **7**, 1648 (1973).
 - [20] G. G. Spink, R. J. Needs, and N. D. Drummond, *Phys. Rev. B* **88**, 085121 (2013).
 - [21] R. P. Feynman, N. Metropolis, and E. Teller, *Phys. Rev.* **75**, 1561 (1949).

- [22] T. Sjoström and J. Daligault, *Phys. Rev. B* **88**, 195103 (2013).
- [23] S. Ma and K. Brueckner, *Phys. Rev.* **165**, 18 (1968).
- [24] K. H. Lau and W. Kohn, *J. Phys. Chem. Solids* **37**, 99 (1976).
- [25] J. P. Perdew, K. Burke, and M. Ernzerhof, *Phys. Rev. Lett.* **77**, 3865 (1996).
- [26] P. Giannozzi *et al.*, *J. Phys.: Condens. Matter* **21**, 395502 (2009).
- [27] S. X. Hu, B. Militzer, V. N. Goncharov, and S. Skupsky, *Phys. Rev. B* **84**, 224109 (2011).
- [28] T. Sjoström and J. Daligault, [arXiv:1407.7051](https://arxiv.org/abs/1407.7051) [Phys. Rev. Lett. (to be published)].